INTERNATIONAL JOURNAL OF PRECISION ENGINEERING AND MANUFACTURING-GREEN TECHNOLOGY Vol. 3, No. 1, pp. 91-97 JANUARY 2016 / 91
DOI: 10.1007/s40684-016-0012-8 ISSN 2288-6206 (Print) / ISSN 2198-0810 (Online)

Frictional Behavior between Silicon and Steel Coated with Graphene Oxide in Dry Sliding and Water Lubrication Conditions

Hae Jin Kim[1], Dong Gap Shin[1], and Dae-Eun Kim[1,#]

1 School of Mechanical Engineering, Yonsei University, 50, Yonsei-ro, Seodaemun-gu, Seoul, 03722, South Korea
Corresponding Author / Email: kimde@yonsei.ac.kr, TEL: +82-2-2123-2822, FAX: +82-2-365-0491

KEYWORDS: Water lubrication, Reduced graphene oxide, Friction, Wear, Green technology

With growing concern over environmental problems, green technologies associated with reducing pollution have been rapidly progressing to attain a sustainable future. Among numerous green technologies currently under development, water lubrication technology that can replace the use of conventional oil lubricants can be a promising technology that may lead to huge benefits with respect to environmental and economic issues. In this work, good-lubricating performance was achieved by using reduced graphene oxide (rGO) coating on AISI 440C stainless steel (SS) ball that was slid against a silicon (Si) specimen under water lubrication condition. Compared to the sliding tests performed in dry condition, the friction coefficient of the rGO coated SS ball slid against the Si specimen under water lubrication condition could be reduced by 12 times. Also, it was shown that friction coefficient of the uncoated SS ball slid against the Si specimen in water and dry conditions were relatively higher than that of the sliding test conducted with the rGO coated SS ball in water lubrication. The experimental results demonstrated that the rGO coating on SS can effectively lower the friction in water lubrication conditions. This work are expected to aid in the development of environmental-friendly lubrication technology for mechanical components.

Manuscript received: August 7, 2015 / Revised: October 11, 2015 / Accepted: October 15, 2015

1. Introduction

Rising concern in environmental issues has strongly motivated the development of green technology with the aim to provide practical means to solve these problems.[1-12] In this regard, water lubrication has received much interest in recent years due to the non-polluting nature of water.[13-19] Though the use of water as a lubricant has received great attention in various applications such as machining processes, the technology has not been fully developed to be used at the industrial scale.[20-24] Nevertheless, given the huge impact of water lubrication on economic benefits and environmental issues, various attempts have been made to realize practical water lubrication technology for various mechanical components.

It has been reported that nitride-based metallic coatings and diamond-like carbon (DLC) coatings showed superior properties in reducing friction and wear under water lubrication condition.[25-27] Wang et al. investigated the tribological properties of TiN(C) coatings with respect to different carbon content under water lubrication condition and showed that a relatively low friction and wear could be attained.[28] Furthermore, Wang et al. demonstrated superior tribological properties of CrN(C) coatings under water lubrication conditions by tuning the content of carbon in the coating during the deposition process.[29] In this regard, it can be stated that the tribological properties of the coating under water lubrication condition are highly dependent on the carbon content in the nitride-based coatings. Furthermore, numerous works on the tribological properties of various DLC based coatings under water lubrication condition were performed. Yamamoto et al. investigated the tribological properties of various hydrogenated DLC coatings with different hardness values under water lubrication condition.[30] It was revealed from the experimental results that the friction and wear properties of DLC coatings and counter surfaces were highly dependent on the hardness of the DLC coating. Also, Wang et al. investigated tribological properties of Ti-DLC coatings with different Ti content under water lubrication condition.[31] It was shown that an optimized content of Ti in the Ti-DLC coating resulted in improved mechanical and tribological properties in water lubrication.

In addition to the realization of water lubrication technology by using metallic hard coatings as mentioned above, inclusion of effective additives such as polymers, biomolecules, metallic nanoparticles, nanodiamonds (NDs) and carbon-based nanoparticles in water was also considered to be a viable solution to acquire superior lubricating performance.[14,32,33] Song et al. demonstrated the reduced friction and wear behaviors of stainless steel by using graphene oxide (GO) and oxide multiwall carbon nanotubes (CNTs-COOH) as additives.[34] It was shown that GO additives in water were more effective in reducing friction and wear compared to the CNTs-COOH additives. Also, it was mentioned that the formation of GO tribofilm on the substrate aided in acquiring superior tribological properties during the sliding tests.

Despite the rapid increase in the interest and high future prospects of water lubrication, the development of efficient and cost effective water lubrication technology is yet to be achieved. In this work, GO coated SS ball fabricated by using the electrodynamic spraying process (ESP) was slid against the Si specimen under water lubrication conditions in order to investigate the lubrication capabilities of the GO coating. Also, uncoated SS balls were slid against the Si specimen in water and dry conditions for comparison. Following the sliding tests, wear tracks formed on the specimen surface were observed by using a scanning electron microscope (SEM, JEOL-6610). From these investigations, the effectiveness of using GO coating on SS surface to achieve low friction under water lubrication conditions was assessed. The following sections describe the details of the experimental work.

2. Experimental Details and Results

2.1 Preparation of GO Coated SS Ball

Prior to the deposition process by using the ESP, graphene oxide (GO) particles were well dispersed in a mixture of H_2O/EtOH solution by using the modified Hummer's method.[35-38] It should be noted that the degree of dispersion in the solution could be considered as one of the important factors in determining the quality of the coating during the ESP.[39] Following the dispersion process of GO in the solution, the thickness and size of a single GO was characterized by using an atomic force microscope (AFM, Park system NX10) as shown in Fig. 1(a). The inset graph in the AFM image shows the surface profile of the region indicated with dotted line. As can be obtained from the surface profile, the size and the thickness of single GO were measured to be about 200 nm and about 1 nm, respectively.

The experimental process was composed of the ESP, reduction treatment and tribo-testing. As for the ESP, GO dispersed solution was supplied to the nozzle by using an injection controller to control the speed of the injection. The injection rate was set to be 5 μL/min. during the ESP. Also, a relatively high voltage was applied to the nozzle by using a power supply in order to generate fine droplets during the ESP. In the ESP, a 2-axis moving stage enabled for the coating to be uniform over a relatively large area. Finally, the GO coating was deposited on the pre-cleaned 1.6 mm 440C SS balls. The GO coating thickness on the SS ball was measured to be about 3 μm by using 3D laser microscope image as shown in Fig. 1(b). Following the ESP, all the samples were placed in the vaporized hydrazine contained glass chamber for 24 hours at 100°C to reduce the GO coating that were deposited on the SS balls.

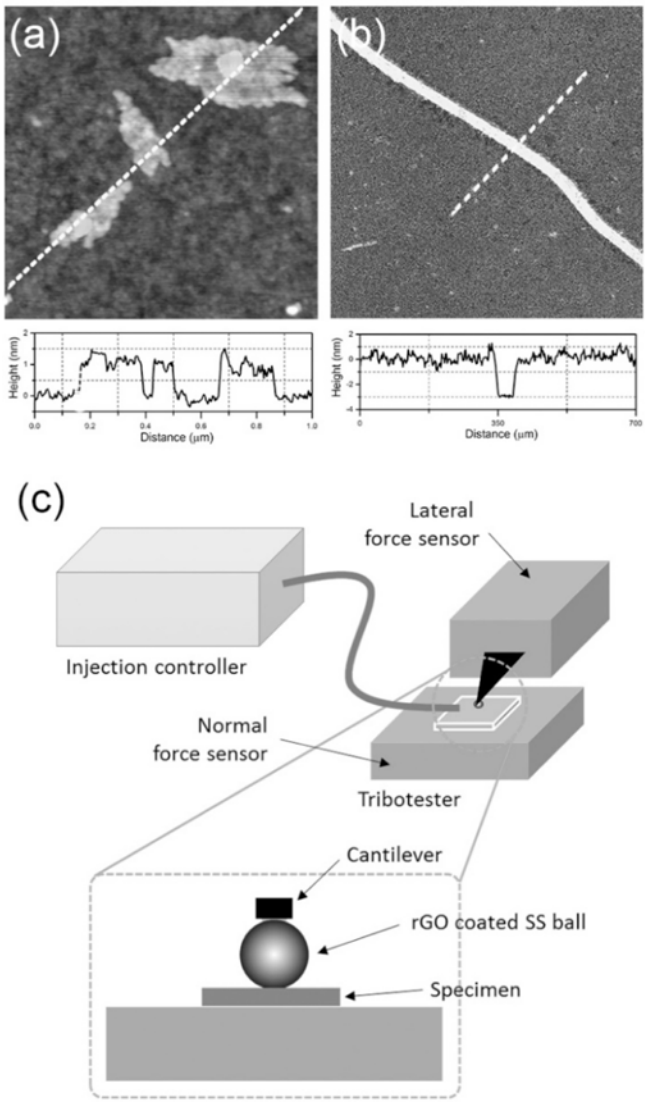

Fig. 1 (a) AFM image of single graphene oxide layer with the 2D surface profile of the region indicated with dotted line. (b) 3D laser microscope image of GO coating on stainless steel ball with 2D surface profile of the region indicated with dotted line (c) Schematic of tribo-testing

The purpose of GO reduction to obtain a reduced graphene oxide (rGO) was to improve the adhesion of the GO coating to the SS ball.

Fig. 1(c) is the schematic showing the experimental set-up used to investigate the friction and wear behaviors of the GO coated SS ball slid against the Si specimen under water lubrication condition. The friction and wear behaviors of the GO coated SS ball were investigated by sliding the balls against the 1 cm × 1 cm^2 Si specimen under water lubrication conditions. In the sliding tests, a reciprocating type of a tribotester was utilized as presented in the schematic of Fig. 1(b). Normal and lateral force sensors (Transducer Techniques, GS0-10) with resolution of 1 mV/V nominal rated output were used to monitor the normal and frictional forces during the sliding tests, respectively. In order to prevent evaporation of water during the sliding tests, water was supplied by using the injection controller with the injection rate of 5 μL/min. In the sliding tests, normal load, sliding stroke and sliding speed

were set to be 20 mN, 2 mm and 4 mm/s (1 Hz), respectively. The 20 mN normal load in the sliding test corresponded to a contact pressure of about 0.28 GPa between SS ball and Si specimen that was calculated by using Hertzian contact pressure equation. All the tests were repeated for three times to assure repeatability of the results. All the tests were performed in an ambient condition inside a Class 100 clean room.

2.2 Friction Behavior of Si in Water and Dry Conditions

Fig. 2(a) shows the friction coefficient with respect to the number of sliding cycles under various sliding conditions. From here on, the GO coating will be referred to as rGO since all the coatings were reduced prior to the sliding tests. It should be noted that rGO-water and rGO-dry sliding conditions represent the experiments in which the rGO coated SS ball was slid against the Si specimen in water lubrication and in dry condition, respectively. Also, SS-water and SS-dry sliding conditions represent the experiments in which the uncoated SS ball was slid against the Si specimen in water lubrication and in dry condition, respectively. As can be confirmed from Fig. 2(a), relatively low friction coefficient of about 0.04 could be obtained for rGO-water sliding condition for 5000 sliding cycles. As for the rGO-dry sliding condition, the friction coefficient was found to be about 0.48 for 5000 sliding cycles. Thus, it can be stated that water had a significant role in reducing the friction force between the rGO coated SS ball and the Si specimen. As for the sliding test conducted under rGO-dry sliding condition, a relatively high friction force was attained due to abrasive wear of the rGO coating on the SS ball against the Si specimen. The particles generated were expected to increase the three-body abrasive interaction at the sliding interface.

In order to investigate the effect of rGO coating on the friction behaviors of SS ball sliding against the Si specimen in water and dry conditions, uncoated SS balls were slid against the Si specimen in water and dry conditions for comparison. It was shown that the friction coefficients of SS-water and SS-dry sliding conditions were about 0.3 and about 0.15, respectively. For the sliding tests conducted under water lubrication condition with and without the rGO coating, it can be concluded that the rGO coating contributed in reducing the friction coefficient by as much as 7.5 times. As for the dry conditions, however, the friction coefficient of the SS-dry sliding condition was shown to be even lower compared to that of the rGO-dry sliding condition. This outcome could be attributed to the generation of numerous abrasive GO wear particles during the sliding test of rGO-dry sliding condition. Moreover, it was observed with the SEM that no wear could be found on the specimens for the SS-dry sliding condition.

It was interesting to note that the friction coefficient of the SS-dry sliding condition was lower than that of the SS-water sliding condition. This outcome implied that pure water cannot be used as a lubricant for SS as previously reported in numerous works.[15,26] Also, compared to the stable friction coefficient for SS-dry sliding condition, relatively unstable friction coefficient of SS-water sliding condition was presumed to be due to the severe wear of the Si specimen. Fig. 2(b) represents the summary of friction coefficient data obtained from the sliding tests under different lubrication conditions. The average friction coefficient for three repeated sliding tests conducted under rGO-water, rGO-dry, SS-water and SS-dry sliding conditions were 0.04 ± 0.001, 0.48 ± 0.15, 0.29 ± 0.03 and 0.15 ± 0.02, respectively. It should be

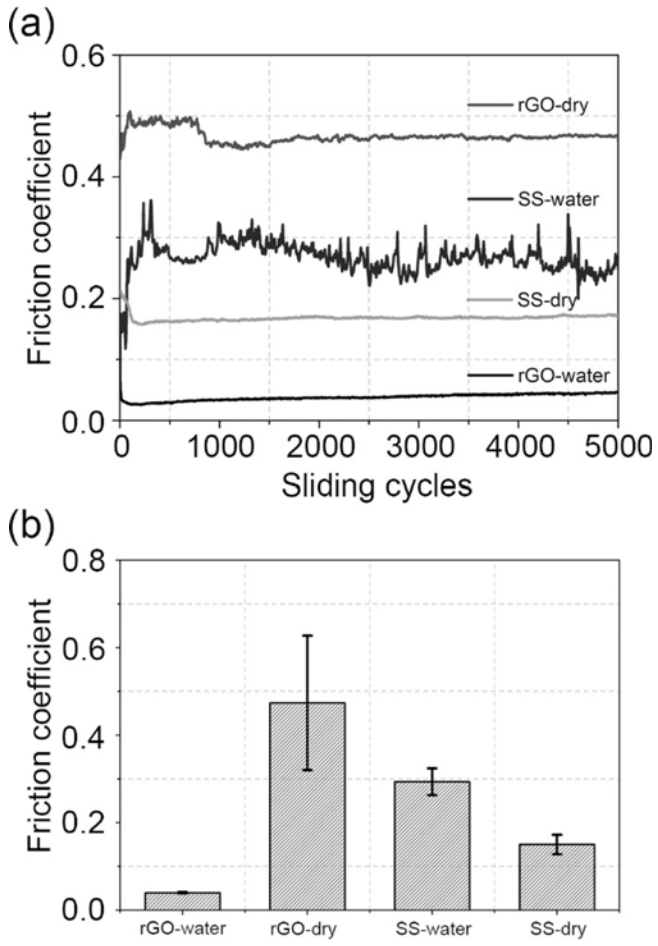

Fig. 2 (a) Friction coefficient of the sliding tests conducted under various sliding conditions. (b) Average friction coefficient of the 3 repeated sliding tests conducted under various sliding conditions. An error bar indicates the standard deviation

mentioned that a relatively large deviation for rGO-dry sliding condition was assumed to be due to the unsteady behavior of the abrasive GO wear particles introduced between the SS ball and the Si specimen during the sliding tests. Overall, it could be determined from the experimental results that the use of rGO coating in water lubrication was effective in reducing the friction force for Si.

2.3 Wear Behaviors of rGO Coated SS Balls in Water and Dry Conditions

Fig. 3 shows the SEM images of the rGO coated and uncoated SS balls after the sliding tests under different lubrication conditions (left) and the magnified SEM images of the contact region (right) indicated with green circle in the SEM images of the balls. Fig. 3(a) shows the SEM images of the rGO coated SS ball after the sliding test under water lubrication condition. It can be noticed from the SEM image of rGO coated SS ball that the rGO coating was delaminated over a large area after the sliding test. Considering that low friction coefficient of about 0.04 was maintained for 5000 sliding cycles for rGO-water sliding condition, it can be stated that the rGO coating was present on the contact region of the SS ball during the sliding tests. Furthermore, since the friction coefficient of the SS-water sliding condition was measured to be about 0.15, it was presumed that the rGO coating was delaminated during the detachment of

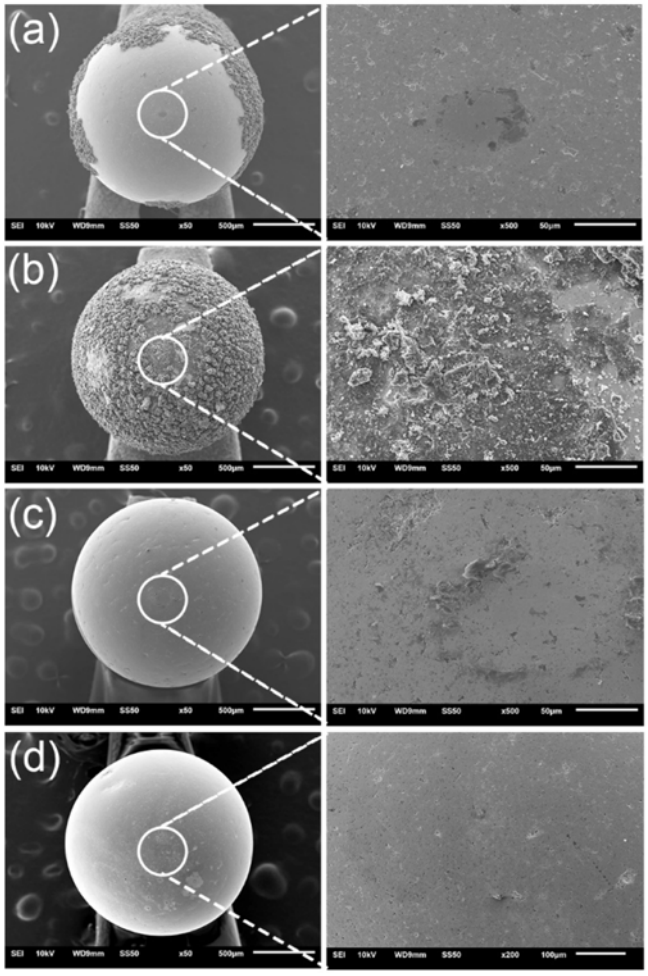

Fig. 3 SEM images of the balls used as counter surface in the sliding tests (left) with the magnified SEM images of the contact region indicated with white circle (right) of (a) rGO coated SS ball slid against Si specimen under water lubrication condition, (b) rGO coated SS ball slid against Si specimen in dry condition, (c) uncoated SS ball slid against Si specimen under water lubrication condition and (d) uncoated SS ball slid against Si specimen in dry condition

the ball after the sliding tests, probably due to the poor adhesion properties between the rGO coating and the SS ball. Furthermore, in the magnified SEM image of the contact region, it can be noticed that a slight amount of rGO was embedded into the SS ball due to relatively high contact pressure experienced during the sliding tests. Overall, it can be concluded that the presence of rGO coating in water lubrication contributed in significantly lowering the friction force between the SS ball and the Si specimen. Fig. 3(b) shows the SEM images of the rGO coated SS ball and the magnified SEM image of the contact region that was slid against the Si specimen in dry condition. As can be seen in Fig. 3(b), the rough surface of rGO coating and numerous rGO abrasive particles present on the surface of the SS ball may have resulted in the relatively high friction coefficient (about 0.48) with large deviations compared to other sliding conditions.

Figs. 3(c) and 3(d) show the SEM images of the uncoated SS balls that were slid against the Si specimen in water and dry conditions, respectively. As for the SS-water sliding condition, it was confirmed from the magnified SEM image of the contact region that a small

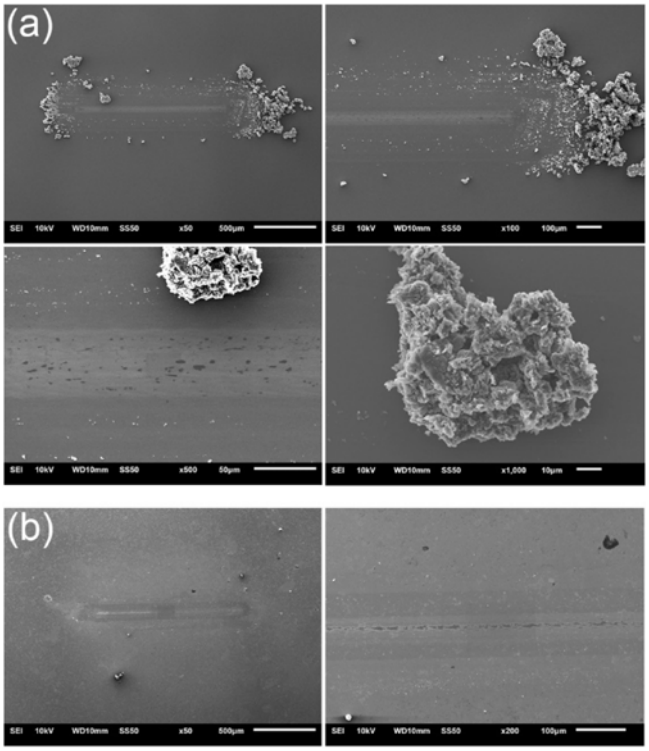

Fig. 4 SEM images of Si specimen after (a) the sliding of rGO coated SS ball against Si specimen in dry condition. (b) The sliding of uncoated SS ball against Si specimen under water lubrication condition

amount of SS wear particles were present on the surface of the SS ball. It may be postulated that these wear particles were generated probably due to the corrosive wear of the SS ball during the sliding tests which led to a relatively high friction coefficient of about 0.29. Unlike the wear particles embedded in the surface of the SS ball for the SS-water sliding condition, relatively clean surface with no apparent wear was observed for the SS ball used in the SS-dry sliding condition as shown in Fig. 3(d).

The wear tracks on the Si specimens were observed by using the SEM as shown in Fig. 4. It should be noted that for the sliding tests conducted with the rGO coated SS ball in water and dry conditions wear tracks were not found and hence, they were not included in Fig. 4. Fig. 4(a) shows the SEM images with different magnifications of the wear track formed on the Si specimen after the sliding test for rGO-dry sliding condition. The SEM images show evidence of many dark particles embedded in the wear track. Considering the fact that the particles were randomly distributed in the wear track, they were thought to be particles that were detached from the GO coating on the SS ball. Thus, these particles were presumed to be GO particles compressed into the wear track during the sliding test. Furthermore, it may be stated that the generation of abrasive GO particles during the sliding tests contributed in attaining a relatively high friction coefficient. Fig. 4(b) shows the SEM images with different magnifications of the wear track formed on the Si specimen after the sliding test for SS-water sliding condition. It can be seen from the magnified SEM image of the wear track (right) in Fig. 4(b) that a number of wear particles were embedded on the wear track. The formation of the wear particles observed on the wear track could also be found on the counter surface (SS ball) as shown in Fig. 3(c). Thus,

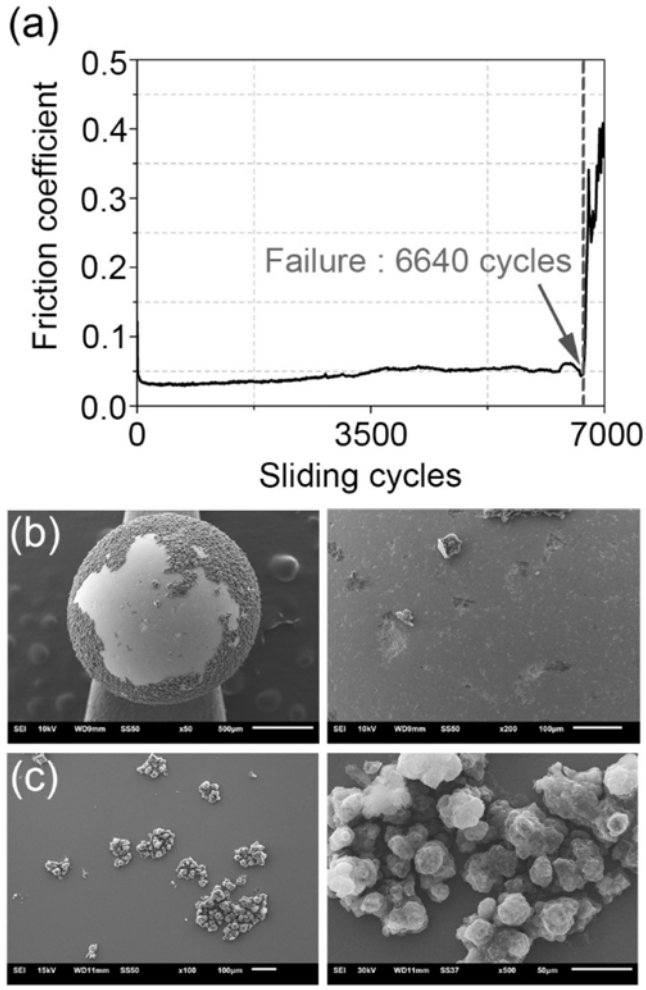

Fig. 5 (a) Friction coefficient of the rGO coated SS ball slid against Si specimen under water lubrication condition with respect to the number of sliding cycles. Grey dotted line in the graph indicate the failure of the rGO coating determined by the rapid increase of friction coefficient. An arrow and the number represents the sliding cycles at the failure. (b) SEM image of rGO coated SS ball (left) with magnified SEM image of contact region (right) after the sliding test under water lubrication condition. (c) SEM images of rGO residue found on the Si specimen after the sliding test due to delamination of the rGO coating on the SS ball

it may be concluded that abrasive wear particles on the wear track resulted in relatively high friction coefficient as presented in Fig. 2(a).

2.4 Durability of the rGO Coated SS Ball

The rGO coated SS ball was slid against Si specimen under water lubrication condition for 7000 sliding cycles to assess the durability of the rGO coating. Fig. 5(a) shows the friction coefficient with respect to the number of sliding cycles for the rGO-water sliding condition. It can be noticed from the graph that the rapid increase in the friction coefficient occurred at 6640 sliding cycles due to the removal of rGO coating. It should be stated that the friction coefficient reached up to about 0.3 due to the absence of the rGO coating between the SS ball and Si specimen, which was consistent with the value obtained from the SS-water sliding condition. Fig. 5(b) shows the SEM images of the rGO coated SS ball after the sliding test (left) with a magnified SEM image of the contact region. It could be observed that large amount of the coating was removed with no evidence of wear on the surface of the SS ball. Fig. 5(c) shows the SEM images with different magnifications of the rGO residue found on the Si specimen after the sliding test. Considering that the morphology of the rGO residues were quite similar to the initial state of the rGO coating on the SS ball, it was reasonable to presume that the coating was delaminated due to poor adhesion between the SS ball and the Si specimen. It was reported in previous works that the water contact angle of both stainless steel and GO coating was -50°.[40,41] As for the rGO coating, the water contact angle was reported to be in the range of 80-90°, indicating relatively low surface energy of the rGO coating.[41] From these data, it may be presumed that the delamination of the rGO coating during the sliding tests was due to low surface energy of the rGO coating. Thus, an improvement of the adhesion property of the rGO coating should be conducted for future work to enhance the durability of the coating in water lubrication.

3. Conclusions

The feasibility of using a SS ball coated with GO to achieve low friction against Si in water lubrication was assessed. The rGO coating was successfully deposited on a SS ball using the ESP followed by the reduction process. The friction and wear behaviors of the rGO coating were assessed by using a reciprocating type of a tribotester in water and dry sliding conditions. The friction coefficient of the rGO coated SS ball sliding against the Si specimen in water lubrication was about 0.04 over 5000 cycles. This value was 12 times lower compared to the friction coefficient (about 0.48) of the rGO coated SS ball sliding against the Si specimen in dry condition. It was found that the friction coefficient of the uncoated SS ball slid against the Si specimen in water and dry conditions were about 0.3 and about 0.15, respectively. Thus, it may be stated that the rGO coating had a significant role in reducing the friction between the SS ball and the Si specimen. Furthermore, it was revealed from the SEM images that the wear of the SS ball slid against the Si specimen under water lubrication condition was significantly lower than that of uncoated SS ball slid against the Si specimen under the same condition. The overall experimental results revealed that that adequate lubricating performance could be derived by using the rGO coated SS ball against Si in water lubrication.

ACKNOWLEDGEMENT

This work was supported by the National Research Foundation of Korea (NRF) grant funded by the Korea government (MSIP) (No. 2010-0018289).

REFERENCES

1. Ahn, S.-H., “An Evaluation of Green Manufacturing Technologies Based on Research Databases,” Int. J. Precis. Eng. Manuf.-Green Tech., Vol. 1, No. 1, pp. 5-9, 2014.

2. Dornfeld, D. A., "Moving towards Green and Sustainable Manufacturing," Int. J. Precis. Eng. Manuf.-Green Tech., Vol. 1, No. 1, pp. 63-66, 2014.

3. Yi, H., Hwang, I., Sung, M., Lee, D., Kim, J.-H., et al., "Bio-Inspired Adhesive Systems for Next-Generation Green Manufacturing," Int. J. Precis. Eng. Manuf.-Green Tech., Vol. 1, No. 4, pp. 347-351, 2014.

4. Kim, H.-J., Yoo, S.-S., and Kim, D.-E. "Nano-Scale Wear: A Review," Int. J. Precis. Eng. Manuf., Vol. 13, No. 9, pp. 1709-1718, 2012.

5. Ahn, S.-H., Chun, D.-M., and Chu, W.-S., "Perspective to Green Manufacturing and Applications," Int. J. Precis. Eng. Manuf., Vol. 14, No. 6, pp. 873-874, 2013.

6. Chu, W.-S., Chun, D.-M., and Ahn, S.-H., "Research Advancement of Green Technologies," Int. J. Precis. Eng. Manuf., Vol. 15, No. 6, pp. 973-977, 2014.

7. Kim, K.-S., Lee, H.-J., Lee, C., Lee, S.-K., Jang, H., et al., "Chemical Vapor Deposition-Grown Graphene: The Thinnest Solid Lubricant," ACS Nano, Vol. 5, No. 6, pp. 5107-5114, 2011.

8. Jang, S., Ahn, J., and Lim, S. H., "Performance of Oil-Separator Adopting Nature-Inspired Surface," Int. J. Precis. Eng. Manuf., Vol. 16, No. 10, pp. 2205-2211, 2015.

9. Kim, Y.-W., Kang, B.-S., and Lee, D.-W., "Improving Efficiency of Dye-Sensitized Solar Cell by Micro Reflectors," Int. J. Precis. Eng. Manuf., Vol. 16, No. 7, pp. 1257-1261, 2015.

10. Lyu, M.-Y. and Choi, T. G., "Research Trends in Polymer Materials for Use in Lightweight Vehicles," Int. J. Precis. Eng. Manuf., Vol. 16, No. 1, pp. 213-220, 2015.

11. Chu, W.-S., Kim, C.-S., Lee, H.-T., Choi, J.-O., Park, J.-I., et al., "Hybrid Manufacturing in Micro/Nano Scale: A Review," Int. J. Precis. Eng. Manuf.-Green Tech., Vol. 1, No. 1, pp. 75-92, 2014.

12. Soubihia, D. F., Jabbour, C. J. C., and Sousa, J. A. B. L., "Green Manufacturing: Relationship between Adoption of Green Operational Practices and Green Performance of Brazilian ISO 9001-Certified Firms," Int. J. Precis. Eng. Manuf.-Green Tech., Vol. 2, No. 1, pp. 95-98, 2015.

13. Chen, C.-Y., Wu, B.-H., Chung, C.-J., Li, W.-L., Chien, C.-W., et al., "Low-Friction Characteristics of Nanostructured Surfaces on Silicon Carbide for Water-Lubricated Seals," Tribology Letters, Vol. 51, No. 1, pp. 127-133, 2013.

14. Kinoshita, H., Nishina, Y., Alias, A. A., and Fujii, M., "Tribological Properties of Monolayer Graphene Oxide Sheets as Water-Based Lubricant Additives," Carbon, Vol. 66, pp. 720-723, 2014.

15. Elomaa, O., Singh, V. K., Iyer, A., Hakala, T. J., and Koskinen, J., "Graphene Oxide in Water Lubrication on Diamond-Like Carbon vs. Stainless Steel High-Load Contacts," Diamond and Related Materials, Vol. 52, pp. 43-48, 2015.

16. Yan, S., Lin, B., Liu, F., and Yan, F., "Friction and Wear of Self-Mated Sic and Si3n4 in Green Water-Based Lubricant," Int. J. Precis. Eng. Manuf., Vol. 13, No. 7, pp. 1067-1072, 2012.

17. Gnanadurai, R. R. and Varadarajan, A., "Investigation on the Effect of an Auxiliary Pulsing Jet of Water at the Top Side of Chip during Hard Turning of Aisi 4340 Steel with Minimal Fluid Application," Int. J. Precis. Eng. Manuf., Vol. 15, No. 7, pp. 1435-1441, 2014.

18. Ye, Y.-S., Zhang, M.-L., and Wang, B.-Y., "Hot-Stamping Die-Cooling System for Vehicle Door Beams," Int. J. Precis. Eng. Manuf., Vol. 14, No. 7, pp. 1251-1255, 2013.

19. Wang, Y.-G., Chen, Y., and Zhao, Y.-W., "Chemical Mechanical Planarization of Silicon Wafers at Natural pH for Green Manufacturing," Int. J. Precis. Eng. Manuf., Vol. 16, No. 9, pp. 2049-2054, 2015.

20. Ohana, T., Suzuki, M., Nakamura, T., Tanaka, A., and Koga, Y., "Low-Friction Behaviour of Diamond-Like Carbon Films in a Water Environment," Diamond and Related Materials, Vol. 15, No. 4, pp. 962-966, 2006.

21. Ding, Q., Wang, L., Wang, Y., Wang, S., Hu, L., et al., "Improved Tribological Behavior of DLC Films under Water Lubrication By Surface Texturing," Tribology Letters, Vol. 41, No. 2, pp. 439-449, 2011.

22. Won, M.-S., Amanov, A., Kim, H.-J., Yun, W.-S., Joo, W.-G., et al., "Evaluation of the Mechanical and Tribological Properties of a TFT-LCD Panel," Tribology International, Vol. 73, No. pp. 95-100, 2014.

23. Wang, Q. J. and Chung, Y.-W., "Encyclopedia of Tribology," Springer, 2013.

24. Park, C., Kim, H., Lee, S., and Jeong, H., "The Influence of Abrasive Size on High-Pressure Chemical Mechanical Polishing of Sapphire Wafer," Int. J. Precis. Eng. Manuf.-Green Tech., Vol. 2, No. 2, pp. 157-162, 2015.

25. Yamamoto, K., Sato, T., and Takeda, M. "Structural Analysis of (Cr 1- x Si x) N Coatings and Tribological Property in Water Environment," Surface and Coatings Technology, Vol. 193, No. 1, pp. 167-172, 2005.

26. Ohana, T., Wu, X., Nakamura, T., and Tanaka, A., "Formation of Lubrication Film of Diamond-Like Carbon Films in Water and Air Environments Against Stainless Steel and Cr-Plated Balls," Diamond and Related Materials, Vol. 16, No. 4, pp. 1336-1339, 2007.

27. Wang, Q., Zhou, F., Chen, K., Wang, M., and Qian, T., "Friction and Wear Properties of TiCN Coatings Sliding Against SiC and Steel Balls in Air and Water," Thin Solid Films, Vol. 519, No. 15, pp. 4830-4841, 2011.

28. Wang, Q., Zhou, F., Zhou, Z., Yang, Y., Yan, C., et al., "Influence of Carbon Content on the Microstructure and Tribological Properties of Tin (C) Coatings in Water Lubrication," Surface and Coatings Technology, Vol. 206, No. 18, pp. 3777-3787, 2012.

29. Wang, Q., Zhou, F., Ding, X., Zhou, Z., Wang, C., et al., "Microstructure and Water-Lubricated Friction and Wear Properties of CrN (C) Coatings with Different Carbon Contents," Applied Surface Science, Vol. 268, pp. 579-587, 2013.

30. Yamamoto, K. and Matsukado, K., "Effect of Hydrogenated DLC Coating Hardness on the Tribological Properties under Water Lubrication," Tribology International, Vol. 39, No. 12, pp. 1609-1614, 2006.

31. Wang, Q., Zhou, F., Zhou, Z., Yang, Y., Yan, C., et al., "Influence of Ti Content on the Structure and Tribological Properties of Ti-DLC Coatings in Water Lubrication," Diamond and Related Materials, Vol. 25, pp. 163-175, 2012.

32. Omotowa, B. A., Phillips, B. S., Zabinski, J. S., and Shreeve, J. N. M., "Phosphazene-Based Ionic Liquids: Synthesis, Temperature-Dependent Viscosity, and Effect as Additives in Water Lubrication of Silicon Nitride Ceramics," Inorganic Chemistry, Vol. 43, No. 17, pp. 5466-5471, 2004.

33. Zhang, C., Zhang, S., Yu, L., Zhang, Z., Wu, Z., et al., "Preparation and Tribological Properties of Water-Soluble Copper/Silica Nanocomposite as a Water-Based Lubricant Additive," Applied Surface Science, Vol. 259, pp. 824-830, 2012.

34. Song, H.-J. and Li, N., "Frictional Behavior of Oxide Graphene Nanosheets as Water-Base Lubricant Additive," Applied Physics A, Vol. 105, No. 4, pp. 827-832, 2011.

35. Berman, D., Erdemir, A., and Sumant, A. V., "Graphene: A New Emerging Lubricant," Materials Today, Vol. 17, No. 1, pp. 31-42, 2014.

36. Penkov, O., Kim, H.-J., Kim, H.-J., and Kim, D.-E., "Tribology of Graphene: A Review," Int. J. Precis. Eng. Manuf., Vol. 15, No. 3, pp. 577-585, 2014.

37. Gong, H. H., Park, S. H., Lee, S.-S., and Hong, S. C., "Facile and Scalable Fabrication of Transparent and High Performance Pt/Reduced Graphene Oxide Hybrid Counter Electrode for Dye-Sensitized Solar Cells," Int. J. Precis. Eng. Manuf., Vol. 15, No. 6, pp. 1193-1199, 2014.

38. Jeon, C.-H., Jeong, Y.-H., Seo, J.-J., Tien, H. N., Hong, S.-T., et al., "Material Properties of Graphene/Aluminum Metal Matrix Composites Fabricated by Friction Stir Processing," Int. J. Precis. Eng. Manuf., Vol. 15, No. 6, pp. 1235-1239, 2014.

39. Kim, H.-J., Penkov, O. V., and Kim, D.-E., "Tribological Properties of Graphene Oxide Nanosheet Coating Fabricated by Using Electrodynamic Spraying Process," Tribology Letters, Vol. 57, No. 3, pp. 1-10, 2015.

40. Kim, M., Song, D., Shin, H., Baeg, S.-H., Kim, G., et al., "Surface Modification for Hydrophilic Property of Stainless Steel Treated by Atmospheric-Pressure Plasma Jet," Surface and Coatings Technology, Vol. 171, No. 1, pp. 312-316, 2003.

41. Some, S., Kim, S., Samanta, K., Kim, Y., Yoon, Y., et al., "Fast Synthesis of High-Quality Reduced Graphene Oxide at Room Temperature under Light Exposure," Nanoscale, Vol. 6, No. 19, pp. 11322-11327, 2014.